Dissipationless Counterflow Currents above T_c in Bilayer Superconductors

Guido Homann,[1] Marios H. Michael,[2,*] Jayson G. Cosme,[3] and Ludwig Mathey[1,4]

[1]*Zentrum für Optische Quantentechnologien und Institut für Quantenphysik, Universität Hamburg, 22761 Hamburg, Germany*
[2]*Max Planck Institute for the Structure and Dynamics of Matter, Luruper Chausse 149, 22761 Hamburg, Germany*
[3]*National Institute of Physics, University of the Philippines, Diliman, Quezon City 1101, Philippines*
[4]*The Hamburg Centre for Ultrafast Imaging, Luruper Chaussee 149, 22761 Hamburg, Germany*

We report the existence of dissipationless currents in bilayer superconductors above the critical temperature T_c, assuming that the superconducting phase transition is dominated by phase fluctuations. Using a semiclassical U(1) lattice gauge theory, we show that thermal fluctuations cause a transition from the superconducting state at low temperature to a resistive state above T_c, accompanied by the proliferation of unbound vortices. Remarkably, while the proliferation of vortex excitations causes dissipation of homogeneous in-plane currents, we find that counterflow currents, flowing in the opposite direction within a bilayer, remain dissipationless. The presence of a dissipationless current channel above T_c is attributed to the inhibition of vortex motion by local superconducting coherence within a single bilayer, in the presence of counterflow currents. Our theory presents a possible scenario for the pseudogap phase in bilayer cuprates.

Introduction.—Underdoped cuprates exhibit two characteristic temperature scales. While these materials are superconducting only below the critical temperature T_c, they feature a gaplike suppression of the density of low-energy electronic states up to a significantly higher temperature T^*. The precise nature of this pseudogap regime is still under debate [1,2]. As the density of superconducting charge carriers is relatively small in underdoped cuprates, it was proposed that the breakdown of superconductivity at T_c is dominated by phase fluctuations [3]. This scenario, in which Cooper pairs exist up to T^*, is consistent with the similarity between the symmetries of the superconducting gap and the pseudogap [4,5]. Remarkably, measurements of the Nernst effect [6–9], magnetization experiments [10,11], and optical spectroscopy [12,13] indicate the existence of superconducting fluctuations well above T_c. Further evidence for superconducting fluctuations in the pseudogap regime is provided by pump-probe experiments involving parametric amplification of Josephson plasmons in $YBa_2Cu_3O_{7-\delta}$ (YBCO) [14–17].

To contribute to the ongoing debate, we investigate the signatures to low-frequency electrodynamics of the phase fluctuating scenario of the pseudogap phase in bilayer superconductors. Specifically, we assume that the transition is dominated by phase fluctuations while the pairing amplitude remains essentially constant up to temperatures close to T^*. We utilize a semiclassical U(1) lattice gauge theory [18–20] to simulate dynamics of the superconducting phase of a bilayer superconductor in the presence of thermal fluctuations. We find a crossover from an ordered state to a highly fluctuating state without global phase coherence at high temperatures, which we associate with the pseudogap phase. Our simulations show that, in the pseudogap phase, long-range coherence is destroyed by the proliferation of vortex excitations, consistent with studies on the anisotropic XY model [21–27]. Prior Berezinskii-Kosterlitz-Thouless studies emphasize the importance of vortices in the phase fluctuation scenario of the pseudogap phase. In this Letter, our simulations add three crucial components absent in previous works: (i) inclusion of the gauge field, (ii) coherent dynamics of fluctuations based on Maxwell's equations, and (iii) accounting for consistent fluctuations and dissipation induced by a thermal bath. The combination of these elements together are vital for accurately simulating low-energy electrodynamics in bilayer superconductors and understanding their collective modes within the pseudogap phase.

We find that the loss of long-range coherence is accompanied by a resistive transition where superconductivity is lost. However, our simulations show that short-range intrabilayer coherence persists far above T_c. A striking consequence of short-range intrabilayer superconducting correlations is that counterflow currents remain dissipationless above T_c. To be precise, the in-plane conductivity of a bilayer superconductor can be divided
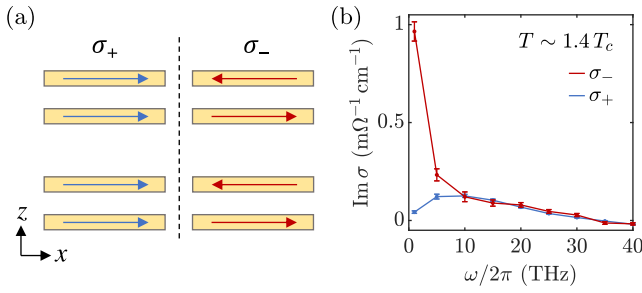
FIG. 1. Dissipationless counterflow in a bilayer superconductor. (a) Current configurations in the copper oxide layers characterized by the symmetric and the antisymmetric conductivity, respectively. (b) Imaginary part of the symmetric and the antisymmetric conductivity at $36\ \mathrm{K} \sim 1.4T_c$. The error bars indicate the standard errors of the ensemble averages.

into a symmetric and an antisymmetric component as depicted in Fig. 1(a). Our simulations, presented in Fig. 1(b), show that the symmetric in-plane conductivity $\sigma_+(\omega)$ no longer features a $1/\omega$ divergence at temperatures $T \gtrsim T_c$, signaling the emergence of a resistive state. In contrast, in-plane currents with opposite direction in the lower and upper layer flow without dissipation. This phenomenon manifests itself in a $1/\omega$ divergence of the antisymmetric conductivity $\sigma_-(\omega)$, as shown in Fig. 1(b). The effect that we present here is conceptually related to a variety of other phenomena, such as antisymmetric quasi-order in a bilayer of superfluids [28], counterflow super-fluidity in cold atoms [29–31], and Bose-Einstein condensation of excitons in bilayer electron systems [32–38]. We clarify that these phenomena are distinct from the normal-superfluid counterflow of the two-fluid model, which occurs within the superfluid phase [39].

Model.—Following the Ginzburg-Landau theory of superconductivity [40], we describe the superconducting state by a complex order parameter $\psi_{\mathbf{r}} = |\psi_{\mathbf{r}}|e^{i\phi_{\mathbf{r}}}$, which is discretized on a three-dimensional lattice with $\mathbf{r}$ being the lattice site. Each superconducting layer is represented by a square lattice as depicted in Fig. 2(a). The crystalline c axis is oriented along the z direction. Because of the Cooper pair charge of $-2e$, the order parameter is coupled to the electromagnetic field. We employ the Peierls substitution such that the electromagnetic vector potential $\mathbf{A_r}$ enters the gauge-invariant phase differences between the lattice sites. The gauge-invariant phase differences, which are defined below, govern the nearest-neighbor tunneling of Cooper pairs.

In our model, we fit our parameters to the bilayer cuprate YBCO [14–16,41,42]. The interlayer distances are d_s for intrabilayer (strong) junctions and d_w for interbilayer (weak) junctions. Here, we choose d_s and d_w such that the interlayer distances approximately reproduce the spacing of CuO_2 layers in the bilayer cuprate YBCO. The in-plane lattice constant d_{ab} is introduced as a short-range cutoff below the in-plane coherence length. The tunneling
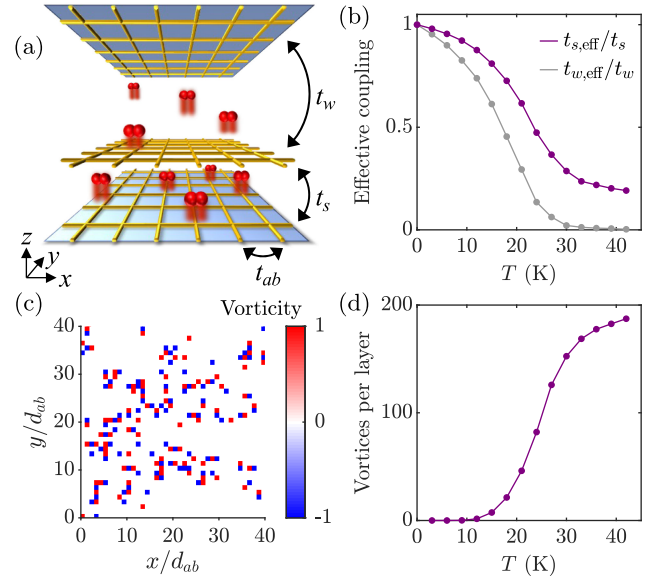
FIG. 2. Semiclassical simulation of a bilayer superconductor. (a) Schematic illustration of the lattice gauge model. (b) Temperature dependence of the effective interlayer tunneling coefficients. The intrabilayer coherence remains nonzero above T_c. (c) Snapshot of the vorticity of the superconducting order parameter at $36\ \mathrm{K} \sim 1.4T_c$. (d) Temperature dependence of the number of vortices per layer. Vortices and antivortices contribute equally to this number. The vortex number rises sharply around T_c, suggesting that the transition is driven by vortex unbinding.

coefficients are t_{ab} for in-plane junctions, t_s for intrabilayer junctions, and t_w for interbilayer junctions. We choose t_s and t_w such that the Josephson plasma frequencies of the simulated bilayer superconductor are comparable to those of YBCO: $\omega_{J1}/2\pi \approx 1$ THz and $\omega_{J2}/2\pi \approx 14$ THz. The in-plane tunneling coefficient t_{ab} determines the in-plane plasma frequency, which we take to be $\omega_{ab}/2\pi \sim 75$ THz at zero temperature.

The Lagrangian and the equations of motion are presented in Supplemental Material [42]. We add Langevin noise and damping terms to the equations of motion and employ periodic boundary conditions. We then integrate the stochastic differential equations using Heun's method with a step size of $\Delta t = 1.25$ as. In the following, we consider a bilayer superconductor with $N_z = 4$ layers and $N_{xy} = 40 \times 40$ sites per layer. The layers $n = 1$ and $n = 2$ form a bilayer, as well as the layers $n = 3$ and $n = 4$. The complete set of model parameters is specified in Supplemental Material [42].

Interlayer phase coherence.—To characterize the coherence of the gauge-invariant intra- and interlayer phase differences, we introduce effective interlayer tunneling coefficients. First, we define the unitless vector potential $a_{j,\mathbf{r}} = -2ed_{j,\mathbf{r}}A_{j,\mathbf{r}}/\hbar$ on the bond between the lattice site $\mathbf{r} \equiv (l, m, n)$ and its nearest neighbor in the $j \in \{x, y, z\}$ direction, where $d_{j,\mathbf{r}}$ denotes the length of the bond. The

gauge-invariant intrabilayer phase differences between layers $n = 1$ and $n = 2$ are $\theta^s_{l,m} = \mathcal{P}(\phi_{l,m,1} - \phi_{l,m,2} + a^z_{l,m,1})$, and the gauge-invariant interbilayer phase differences between layers $n = 2$ and $n = 3$ are $\theta^w_{l,m} = \mathcal{P}(\phi_{l,m,2} - \phi_{l,m,3} + a^z_{l,m,2})$. Note that the gauge-invariant phase differences are mapped onto the interval $(-\pi, \pi]$ by the projection operator $\mathcal{P}(\cdot)$. In the presence of thermal fluctuations, we determine the effective interlayer tunneling coefficients

$$t_{s,\mathrm{eff}} = t_s \langle \cos \theta^s_{l,m} \rangle, \qquad (1)$$

$$t_{w,\mathrm{eff}} = t_w \langle \cos \theta^w_{l,m} \rangle. \qquad (2)$$

The temperature dependence of the effective tunneling coefficients is shown in Fig. 2(b), where we average the cosine of the interlayer phase differences over the xy plane, for a time interval of 2 ps, and an ensemble of 100 trajectories. The onset of strong phase fluctuations dramatically suppresses the interbilayer tunneling coefficient around a crossover temperature of 25 K, which we take to be the transition temperature T_c. While the advent of strong phase fluctuations suppresses also the intrabilayer coefficient t_s, it remains nonzero up to large temperatures. This indicates that, while long-range order is lost across the transition, the pseudogap phase still retains strong local phase coherence within each bilayer. The consequences of phase fluctuations on the plasma resonances as well as the temperature dependence of the in-plane tunneling coefficient and the amplitude of the order parameter in our model are presented in Supplemental Material [42].

Vortices.—To understand the microscopic nature of the phase transition, we turn our attention to the role of vortices in the pseudogap phase. In continuum theories, a vortex is defined through the phase winding of the order parameter along a closed path:

$$\Phi = \oint \boldsymbol{\nabla}\phi \cdot d\mathbf{r} = \oint \left(\boldsymbol{\nabla}\phi + \frac{2e}{\hbar}\mathbf{A} \right) \cdot d\mathbf{r} - \oint \frac{2e}{\hbar}\mathbf{A} \cdot d\mathbf{r}. \qquad (3)$$

In our simulation, we use the latter representation, as it is based on quantities that directly enter the Lagrangian. We define the vorticity of a single plaquette in the xy plane as

$$\begin{aligned} v_{l,m,n} = &\frac{1}{2\pi}\left(a^x_{l,m,n} + a^y_{l+1,m,n} - a^x_{l,m+1,n} - a^y_{l,m,n} \right) \\ &- \frac{1}{2\pi}\left(\theta^x_{l,m,n} + \theta^y_{l+1,m,n} - \theta^x_{l,m+1,n} - \theta^y_{l,m,n} \right), \end{aligned} \qquad (4)$$

where $\theta^x_{l,m,n} = \mathcal{P}(\phi_{l,m,n} - \phi_{l+1,m,n} + a^x_{l,m,n})$ and $\theta^y_{l,m,n} = \mathcal{P}(\phi_{l,m,n} - \phi_{l,m+1,n} + a^y_{l,m,n})$. The vorticity can assume the values -1, 0, and $+1$. A vorticity of $+1$

corresponds to a vortex, while a vorticity of -1 corresponds to an antivortex.

In Fig. 2(c), we show a snapshot of the vorticity in the lowest layer at a temperature of 36 K $\sim 1.4T_c$. Even though most vortex and antivortex form pairs or clusters (seen as blue and red squares next to each other), we crucially also find isolated vortices and antivortices, indicating that the phase transition is driven by vortex-antivortex unbinding. In Fig. 2(d), we plot the number of vortices per layer as a function of temperature. The number of vortices exhibits a rapid increase between 15 and 30 K. Details of the behavior of vortices in the pseudogap phase are captured by computing in-plane and out-of plane correlations, which can be found in Supplemental Material [42]. In addition, the presence of vortices leads to a disordered Josephson intrabilayer potential. The strength and spectral behavior of the vortex-induced disorder is also presented in Supplemental Material [42]. Here, we focus on the consequences of the phase transition on the conductivity.

In-plane conductivity.—We separate the in-plane conductivity of a bilayer superconductor into a symmetric and an antisymmetric component as shown in Fig. 1(a). To calculate the two components of the conductivity, we introduce an oscillating symmetric (antisymmetric) current, $J_\pm$. Once a steady state is reached, we compute $\sigma_\pm(\omega) = J_\pm(\omega)/E_\pm(\omega)$, where $E_\pm$ is the symmetric (antisymmetric) electric field. Details of the conductivity measurements are provided in Supplemental Material [42].

The symmetric and the antisymmetric conductivity are shown for different temperatures in Fig. 3. At a temperature of 15 K $\sim 0.6T_c$, σ_+ and σ_- are in good agreement with each other. The imaginary part of σ_+ and σ_- exhibits the characteristic $1/\omega$ behavior of a superconductor. While the real part of both conductivities is relatively flat for frequencies above 10 THz, it tends to slowly increase with decreasing frequency below 10 THz. The values of $\mathrm{Re}\sigma_+$ and $\mathrm{Re}\sigma_-$ at 1 THz bear some uncertainty due to slow numerical convergence.

At temperatures $T \gtrsim T_c$, the phase transition is accompanied by a dissipative transition, where the imaginary part of σ_+ no longer diverges as $1/\omega$. At temperatures close to T_c, the real part of σ_+ rises significantly at small frequencies. By contrast, the imaginary part of σ_- exhibits a $1/\omega$ divergence up to temperatures well above T_c while the real part has no significant temperature dependence. This manifestation of remnant superconductivity above T_c is the key result of the present work.

Origin of dissipationless counterflow.—The breakdown of the $1/\omega$ divergence of the imaginary part of σ_+ reveals a transition to a resistive state at T_c. This indicates an unbinding of planar vortex-antivortex pairs above T_c, similar to the resistive transition in superconducting thin films [50,51]. The underlying mechanism of this transition is the following. In the presence of a current $\mathbf{J}$, a single vortex is exposed to a Magnus force $\mathbf{F} = \mathbf{J} \times \boldsymbol{\Phi_0}$, where $\boldsymbol{\Phi_0}$
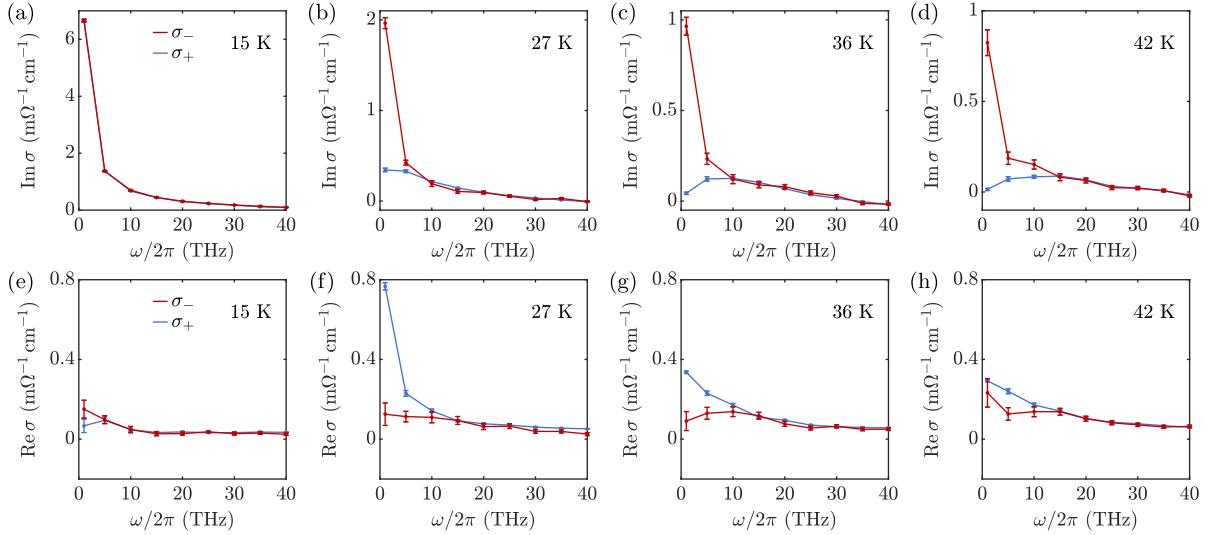
FIG. 3. Symmetric and antisymmetric conductivity at different temperatures. (a)–(d) Imaginary part. (e)–(h) Real part. The error bars indicate the standard errors of the ensemble averages. The crossover temperature is $T_c \sim 25$ K. The antisymmetric conductivity indicates superconductivity above T_c.

has the magnitude of a flux quantum $\Phi_0 = \pi\hbar/e$ and points in the direction of the magnetic field inside the vortex core. In the case of a dc current, unbound vortices and antivortices drift in opposite directions perpendicular to the current, dissipating energy.

The simultaneous observation of dissipationless counterflow suggests that unbound vortex lines cut through an entire bilayer rather than just a single layer. Equivalently, a vortex in one layer of a bilayer is paired with a vortex of the same vorticity in the other layer of the same bilayer. In this scenario, the dissipation of currents in the two layers of the same bilayer is different, depending on whether the currents flow in the same or opposite directions. If the currents flow in the same direction, the Magnus force points in the same direction for all vortices in the two layers with the same vorticity. Thus, each vortex-vortex pair experiences a drift
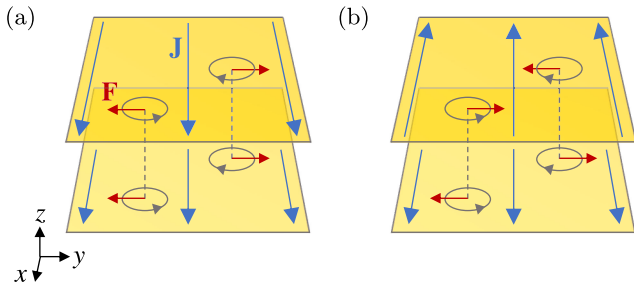
FIG. 4. Dynamics of intrabilayer vortex pairs in the presence of in-plane currents, sustaining dissipationless counterflow. (a) Vortex dynamics in the presence of unidirected in-plane currents. (b) Vortex dynamics in the presence of counterdirected in-plane currents. Vortices in different superconducting layers within the same bilayer are pinned relative to each other due to the residual superconducting coherence within a single bilayer.

motion perpendicular to the current direction as depicted in Fig. 4(a). Analogously to the case of a thin film, the vortex motion dissipates energy, implying a nonzero resistivity. If the currents flow in opposite directions, however, the Magnus force points into opposite directions for the two vortices of each intrabilayer pair. The remnant intrabilayer coherence leads to an effective potential with a linear dependence on the pair size, acting as string tension against the flow of the two vortices away from each other in the presence of counterflow currents [52]. Thus, the intrabilayer vortex pairs experience no net force as highlighted by Fig. 4(b). Since the vortices do not move in this case, the flow of counterdirected currents is dissipationless, consistent with the observation of a $1/\omega$ divergence of the imaginary part of σ_- above T_c.

We note that the previous paragraph provides only a simplified description of the vortex dynamics in the presence of in-plane currents. In fact, the vortex dynamics is very complicated due to the high density of vortices in the layers and fast creation and annihilation processes; see Supplemental Material [42]. Nonetheless, the scenario of intrabilayer vortex-vortex pairs that are essentially unbound from any antivortices is supported by several correlation functions [42]. In Supplemental Material, we also calculate conductivities at finite momentum along the z direction [42]. The results are momentum independent, which corroborates the picture of decoupled bilayers, where vortex lines between different bilayers are uncorrelated.

Conclusion.—We have discovered that counterflow currents flow without dissipation even above the phase transition temperature in a U(1) gauge-invariant model for bilayer superconductors coupled to a thermal bath. Experimental verification of the existence of dissipationless counterflow in bilayer cuprates would provide smoking

gun evidence that the pseudogap phase in bilayer superconductors corresponds to phase-fluctuating superconductivity with strong intrabilayer superconducting correlations up to high temperatures. Importantly, the observation of dissipationless counterflow currents would strongly support the scenario of preformed pairs without global phase coherence as the correct description of the pseudogap phase, in general, applying also to monolayer cuprate superconductors. We expect counterflow currents to appear when a magnetic field is applied in parallel to the layers, giving rise to a diamagnetic response [53]. The results presented here open up interesting research questions about the full range of consequences of such dissipationless currents and whether they can be technologically exploited.

*Corresponding author: marios.michael@mpsd.mpg.de

[1] M. R. Norman, D. Pines, and C. Kalli, The pseudogap: Friend or foe of high T_c?, Adv. Phys. **54**, 715 (2005).

[2] B. Keimer, S. A. Kivelson, M. R. Norman, S. Uchida, and J. Zaanen, From quantum matter to high-temperature superconductivity in copper oxides, Nature (London) **518**, 179 (2015).

[3] V. J. Emery and S. A. Kivelson, Importance of phase fluctuations in superconductors with small superfluid density, Nature (London) **374**, 434 (1995).

[4] A. Damascelli, Z. Hussain, and Z.-X. Shen, Angle-resolved photoemission studies of the cuprate superconductors, Rev. Mod. Phys. **75**, 473 (2003).

[5] M. Hashimoto, I. M. Vishik, R.-H. He, T. P. Devereaux, and Z.-X. Shen, Energy gaps in high-transition-temperature cuprate superconductors, Nat. Phys. **10**, 483 (2014).

[6] Z. A. Xu, N. P. Ong, Y. Wang, T. Kakeshita, and S. Uchida, Vortex-like excitations and the onset of superconducting phase fluctuation in underdoped $La_{2-x}Sr_xCuO_4$, Nature (London) **406**, 486 (2000).

[7] Y. Wang, L. Li, and N. P. Ong, Nernst effect in high-T_c superconductors, Phys. Rev. B **73**, 024510 (2006).

[8] R. Daou, J. Chang, D. LeBoeuf, O. Cyr-Choinière, F. Laliberté, N. Doiron-Leyraud, B. J. Ramshaw, R. Liang, D. A. Bonn, W. N. Hardy, and L. Taillefer, Broken rotational symmetry in the pseudogap phase of a high-T$_c$ superconductor, Nature (London) **463**, 519 (2010).

[9] O. Cyr-Choinière *et al.*, Pseudogap temperature T^* of cuprate superconductors from the Nernst effect, Phys. Rev. B **97**, 064502 (2018).

[10] Y. Wang, L. Li, M. J. Naughton, G. D. Gu, S. Uchida, and N. P. Ong, Field-enhanced diamagnetism in the pseudogap state of the cuprate $Bi_2Sr_2CaCu_2O_{8+\delta}$ superconductor in an intense magnetic field, Phys. Rev. Lett. **95**, 247002 (2005).

[11] L. Li, Y. Wang, S. Komiya, S. Ono, Y. Ando, G. D. Gu, and N. P. Ong, Diamagnetism and Cooper pairing above T_c in cuprates, Phys. Rev. B **81**, 054510 (2010).

[12] J. Corson, R. Mallozzi, J. Orenstein, J. N. Eckstein, and I. Bozovic, Vanishing of phase coherence in underdoped $Bi_2Sr_2CaCu_2O_{8+\delta}$, Nature (London) **398**, 221 (1999).

[13] A. Dubroka, M. Rössle, K. W. Kim, V. K. Malik, D. Munzar, D. N. Basov, A. A. Schafgans, S. J. Moon, C. T. Lin, D. Haug, V. Hinkov, B. Keimer, T. Wolf, J. G. Storey, J. L. Tallon, and C. Bernhard, Evidence of a precursor superconducting phase at temperatures as high as 180 K in $RBa_2Cu_3O_{7-\delta}$ ($R = Y, Gd, Eu$) superconducting crystals from infrared spectroscopy, Phys. Rev. Lett. **106**, 047006 (2011).

[14] W. Hu, S. Kaiser, D. Nicoletti, C. R. Hunt, I. Gierz, M. C. Hoffmann, M. Le Tacon, T. Loew, B. Keimer, and A. Cavalleri, Optically enhanced coherent transport in $YBa_2Cu_3O_{6.5}$ by ultrafast redistribution of interlayer coupling, Nat. Mater. **13**, 705 (2014).

[15] S. Kaiser, C. R. Hunt, D. Nicoletti, W. Hu, I. Gierz, H. Y. Liu, M. Le Tacon, T. Loew, D. Haug, B. Keimer, and A. Cavalleri, Optically induced coherent transport far above T_c in underdoped $YBa_2Cu_3O_{6+\delta}$, Phys. Rev. B **89**, 184516 (2014).

[16] A. von Hoegen, M. Fechner, M. Först, N. Taherian, E. Rowe, A. Ribak, J. Porras, B. Keimer, M. Michael, E. Demler, and A. Cavalleri, Amplification of superconducting fluctuations in driven $YBa_2Cu_3O_{6+x}$, Phys. Rev. X **12**, 031008 (2022).

[17] M. H. Michael, A. von Hoegen, M. Fechner, M. Först, A. Cavalleri, and E. Demler, Parametric resonance of Josephson plasma waves: A theory for optically amplified interlayer superconductivity in $YBa_2Cu_3O_{6+x}$, Phys. Rev. B **102**, 174505 (2020).

[18] G. Homann, J. G. Cosme, and L. Mathey, Higgs time crystal in a high-T_c superconductor, Phys. Rev. Res. **2**, 043214 (2020).

[19] G. Homann, J. G. Cosme, J. Okamoto, and L. Mathey, Higgs mode mediated enhancement of interlayer transport in high-T_c cuprate superconductors, Phys. Rev. B **103**, 224503 (2021).

[20] G. Homann, J. G. Cosme, and L. Mathey, Parametric control of Meissner screening in light-driven superconductors, New J. Phys. **24**, 113007 (2022).

[21] L. I. Glazman and A. E. Koshelev, Critical behavior of layered superconductors, Sov. Phys. JETP **70**, 774 (1990).

[22] W. Janke and T. Matsui, Crossover in the XY model from three to two dimensions, Phys. Rev. B **42**, 10673 (1990).

[23] P. Minnhagen and P. Olsson, Crossover to effectively two-dimensional vortices for high-T_c superconductors, Phys. Rev. Lett. **67**, 1039 (1991).

[24] P. Minnhagen and P. Olsson, Monte Carlo calculation of the vortex interaction for high-T_c superconductors, Phys. Rev. B **44**, 4503 (1991).

[25] D. S. Fisher, M. P. A. Fisher, and D. A. Huse, Thermal fluctuations, quenched disorder, phase transitions, and

transport in type-II superconductors, Phys. Rev. B **43,** 130 (1991).

[26] Y. Matsuda, S. Komiyama, T. Onogi, T. Terashima, K. Shimura, and Y. Bando, Thickness dependence of the Kosterlitz-Thouless transition in ultrathin $yba_2cu_3o_{7-\delta}$ films, Phys. Rev. B **48,** 10498 (1993).

[27] B. Chattopadhyay and S. R. Shenoy, Kosterlitz-Thouless signatures from 3D vortex loops in layered superconductors, Phys. Rev. Lett. **72,** 400 (1994).

[28] L. Mathey, A. Polkovnikov, and A. H. Castro Neto, Phase-locking transition of coupled low-dimensional superfluids, Europhys. Lett. **81,** 10008 (2008).

[29] A. Hu, L. Mathey, I. Danshita, E. Tiesinga, C. J. Williams, and C. W. Clark, Counterflow and paired superfluidity in one-dimensional Bose mixtures in optical lattices, Phys. Rev. A **80,** 023619 (2009).

[30] A. Hu, L. Mathey, E. Tiesinga, I. Danshita, C. J. Williams, and C. W. Clark, Detecting paired and counterflow superfluidity via dipole oscillations, Phys. Rev. A **84,** 041609(R) (2011).

[31] A. B. Kuklov and B. V. Svistunov, Counterflow superfluidity of two-species ultracold atoms in a commensurate optical lattice, Phys. Rev. Lett. **90,** 100401 (2003).

[32] J. P. Eisenstein, G. S. Boebinger, L. N. Pfeiffer, K. W. West, and S. He, New fractional quantum Hall state in double-layer two-dimensional electron systems, Phys. Rev. Lett. **68,** 1383 (1992).

[33] E. Tutuc, M. Shayegan, and D. A. Huse, Counterflow measurements in strongly correlated GaAs hole bilayers: Evidence for electron-hole pairing, Phys. Rev. Lett. **93,** 036802 (2004).

[34] J. P. Eisenstein and A. H. MacDonald, Bose-Einstein condensation of excitons in bilayer electron systems, Nature (London) **432,** 691 (2004).

[35] J.-J. Su and A. H. MacDonald, How to make a bilayer exciton condensate flow, Nat. Phys. **4,** 799 (2008).

[36] E. Babaev, Vortex matter, effective magnetic charges, and generalizations of the dipolar superfluidity concept in layered systems, Phys. Rev. B **77,** 054512 (2008).

[37] Y. Joglekar, D. K. K. Lee, P. R. Eastham, and N. R. Cooper, Breakdown of counterflow superfluidity in a disordered quantum Hall bilayer, Adv. Condens. Matter Phys. **2011,** 792125 (2011).

[38] A. V. Balatsky, Y. N. Joglekar, and P. B. Littlewood, Dipolar superfluidity in electron-hole bilayer systems, Phys. Rev. Lett. **93,** 266801 (2004).

[39] H. Kobayashi, S. Yui, and M. Tsubota, Numerical study on entrance length in thermal counterflow of superfluid ^{4}He, J. Low Temp. Phys. **196,** 35 (2019).

[40] V. L. Ginzburg and L. D. Landau, On the theory of superconductivity, Zh. Eksp. Teor. Fiz. **20,** 1064 (1950).

[41] N. Sellati, F. Gabriele, C. Castellani, and L. Benfatto, Generalized Josephson plasmons in bilayer superconductors, Phys. Rev. B **108,** 014503 (2023).

[42] See Supplemental Material at http://link.aps.org/supplemental/10.1103/PhysRevLett.132.096002 for details on the lattice gauge model, model parameters, the temperature dependence of the in-plane tunneling and the superconducting order parameter, information on the plasma resonances, vortex correlations, and details on the conductivity measurements, which includes Refs. [43–49].

[43] M. Machida, T. Koyama, and M. Tachiki, Dynamical breaking of charge neutrality in intrinsic Josephson junctions: Common origin for microwave resonant absorptions and multiple-branch structures in the $I - V$ characteristics, Phys. Rev. Lett. **83,** 4618 (1999).

[44] D. van der Marel and A. A. Tsvetkov, Transverse-optical Josephson plasmons: Equations of motion, Phys. Rev. B **64,** 024530 (2001).

[45] T. Koyama, Josephson plasma resonances and optical properties in high-T_c superconductors with alternating junction parameters, J. Phys. Soc. Jpn. **71,** 2986 (2002).

[46] T. Koyama and M. Tachiki, $I - V$ characteristics of Josephson-coupled layered superconductors with longitudinal plasma excitations, Phys. Rev. B **54,** 16183 (1996).

[47] M. Machida and T. Koyama, Localized rotating-modes in capacitively coupled intrinsic Josephson junctions: Systematic study of branching structure and collective dynamical instability, Phys. Rev. B **70,** 024523 (2004).

[48] H. Shibata and T. Yamada, Double Josephson plasma resonance in T^* phase $SmLa_{1-x}Sr_xCuO_{4-\delta}$, Phys. Rev. Lett. **81,** 3519 (1998).

[49] T. Schneider and E. Stoll, Molecular-dynamics study of structural-phase transitions. I. One-component displacement models, Phys. Rev. B **13,** 1216 (1976).

[50] B. Halperin and D. Nelson, Resistive transition in superconducting films, J. Low Temp. Phys. **36,** 599 (1979).

[51] P. Minnhagen, The two-dimensional Coulomb gas, vortex unbinding, and superfluid-superconducting films, Rev. Mod. Phys. **59,** 1001 (1987).

[52] S. M. Girvin and A. H. MacDonald, Multicomponent quantum Hall systems: The sum of their parts and more, in *Perspectives in Quantum Hall Effects* (John Wiley & Sons, New York, 1996), Chap. 5, pp. 161–224.

[53] F. Yu, M. Hirschberger, T. Loew, G. Li, B. J. Lawson, T. Asaba, J. B. Kemper, T. Liang, J. Porras, G. S. Boebinger, J. Singleton, B. Keimer, L. Li, and N. P. Ong, Magnetic phase diagram of underdoped $YBa_2Cu_3O_y$ inferred from torque magnetization and thermal conductivity, Proc. Natl. Acad. Sci. U.S.A. **113,** 12667 (2016).